CHEMISTRY OF MATERIALS
Article

Chem. Mater. **2010,** *22,* 1521–1532 1521
DOI:10.1021/cm903557e

Self-Assembled Structures of Semiconductor Nanocrystals and Polymers for Photovoltaics. 2. Multilayers of CdSe Nanocrystals and Oligo(poly)thiophene-Based Molecules. Optical, Electrochemical, Photoelectrochemical, and Photoconductive Properties.

G. Zotti* and B. Vercelli

Istituto CNR per l' Energetica e le Interfasi c.o Stati Uniti 4, 35127 Padova, Italy

A. Berlin

Istituto CNR di Scienze e Tecnologie Molecolari via C.Golgi 19, 20133 Milano, Italy

M. Pasini

Istituto CNR per lo Studio delle Macromolecole via E.Bassini 15, 20133 Milano, Italy

T.L. Nelson and R.D. McCullough

Department of Chemistry, Carnegie Mellon University 4400 Fifth Ave, Pittsburgh, Pennsylvania 15213

T. Virgili

IFN-CNR, c/o Dipartimento di Fisica, Politecnico di Milano P.zza Leonardo da Vinci 32, 20132 Milano, Italy

Received September 9, 2009. Revised Manuscript Received January 12, 2010

A series of terthiophene and sexithiophene α,ω-dicarboxylic and -diphosphonic acids and some poly(thiophene-carboxylate)s and -sulfonate)s were reacted with hexadecylamine-capped CdSe nanoparticles (6 or 7.5 nm diameter) in $CHCl_3$ to form regular polymeric structures on ITO-glass surfaces via layer-by-layer (LBL) alternation. The new materials were investigated by cyclic voltammetry, UV−vis, FTIR and PL spectroscopy, photoelectrochemistry, and photoconductivity. The LBL structures, constituted by quantum dots linked by hole-transporting conjugated chains, display optical and electronic properties useful in photovoltaic devices. The conjugated linker chains ease in fact charge transport between dots but transport of photogenerated carriers is dominated by interdot distance.

1. Introduction

Conjugated polymers (CPs) are organic semiconductors that combine tunable electro-optical properties with a high degree of processability.[1] Inorganic nanocrystals (NCs) are another interesting class of low-dimensional, semiconducting materials[2] which show a distinctive size dependence of the absorption and emission energy due to the quantum confinement effect, giving rise to properties between those of the molecule and the bulk.[3] The integration of inorganic semiconductor nanoparticles and organic conjugated polymers leads to composite materials with interesting physical properties.[4] Their characteristics are promising for applications in light-emitting diodes, photovoltaics, photorefractions, lasers, and biosensors.[5]

There has recently been a considerable interest in the development of photovoltaic devices in which the active

*To whom correspondence should be addressed. Phone: (39)049-829-5868. Fax: (39)049-829-5853. E-mail: g.zotti@ieni.cnr.it.

(1) (a) *Handbook of Organic Conductive Molecules and Polymers*; Nalwa, H. S., Ed.; Wiley: New York, 1997. (b) Kraft, A.; Grimsdale, A. C.; Holmes, A. B. *Angew. Chem., Int. Ed.* **1998**, *37*, 402. (c) *Semiconducting Polymers: Chemistry, Physics,and Engineering*; Hadziioannou, G., van Hutten, P. F., Eds.; Wiley-VCH: Weinheim, Germany, 2000.

(2) *Low-Dimensional Semiconductor Structures: Fundamentals and Device Applications*; Barnham, K., Vvedensky, D., Eds.; Cambridge University Press: Cambridge, U.K., 2001.

(3) (a) Murray, C. B.; Norris, D. J.; Bawendi, M. G. *J. Am. Chem. Soc.* **1993**, *115*, 8706. (b) Alivisatos, A. P. *J. Phys. Chem.* **1996**, *100*, 13 226. (c) Nirmal, M.; Brus, L. *Acc. Chem. Res.* **1999**, *32*, 407. (d) Murray, C. B.; Kagan, C. R.; Bawendi, M. G. *Annu. Rev. Mater. Sci.* **2000**, *30*, 545.

(4) (a) Gangopadhyay, R.; De, A. *Chem. Mater.* **2000**, *12*, 608. (b) Godovvsky, D. Y. *Adv. Polym. Sci.* **2000**, *153*, 163.

(5) (a) Colvin, V. L.; Schlamp, M. C.; Alivisatos, A. P. *Nature* **1994**, *370*, 534. (b) Dabbousi, B. O.; Bawendi, M. G.; Onitsuka, O.; Rubner, M. F. *Appl. Phys. Lett.* **1995**, *66*, 1316. (c) Schlamp, M. C.; Peng, X.; Alivisatos, A. P. *J. Appl. Phys.* **1997**, *82*, 5837. (d) Huynh, W. U.; Peng, X.; Alivisatos, A. P. *Adv. Mater.* **1999**, *11*, 923. (e) Suh, D. J.; Park, O O.; Ahn, T.; Shim, H.-K. *Opt. Mater.* **2002**, *21*, 365. (f) Kamat, P. V. *J. Phys. Chem. C* **2008**, *112*, 18737.

Published on Web 01/25/2010

matrix consists of CPs,[6] motivated by the potential of organic polymers to offer economic viability for solar energy conversion owing to their low cost, ease of processing, and lightweight. High efficiency of optical-to-electrical power conversion has been achieved in cells fabricated using organic−inorganic hybrid structures, in which inorganic semiconductor nanocrystals are introduced to utilize their high electron mobility and overcome charge-transport limitations associated with organic materials.[7] A specific and well-known example is a device in which elongated cadmium selenide nanocrystals (CdSe-NCs) are mixed with poly-3-hexylthiophene, (P3HT) and sandwiched between aluminum and indium−tin-oxide electrodes to create a device with a power conversion efficiency of 1.7%.[8]

Difficulties are in any case still encountered in charge transport between NCs. They may in principle be coated and connected with an electroactive surfactant designed to facilitate their electronic interaction as in gold nanocrystals with electron transport mediated by conjugated thiols.[9] Charge transfer at the organic−inorganic interface may in fact occur rapidly, but only on condition that no insulating monolayer lies at the interface.[10] Thus there is a significant need for fast transfer between inorganic and organic semiconductors, and this concerns *both electron and hole transport*. In fact if we consider bulk heterojunction (BHJ) solar cells, which currently have efficiencies of 5%, blends of a semiconducting polymer (usually an electron donor) and an electron acceptor phase-separate on the nanoscale, as in the above-mentioned case of CdSe and P3HT. In such cases the polymer is the hole-carrying sensitizer and electron-transport operates in CdSe. On the contrary in dye-sensitized solar cell (DSSC), the efficiency of which currently tops out at ~11%, the electron-carrying TiO_2 is sensitized by CdSe-NCs[11] where hole-transport is most likely operating.

Scheme 1. Energy Level Diagram for CdSe-NCs and Oligothiophenes

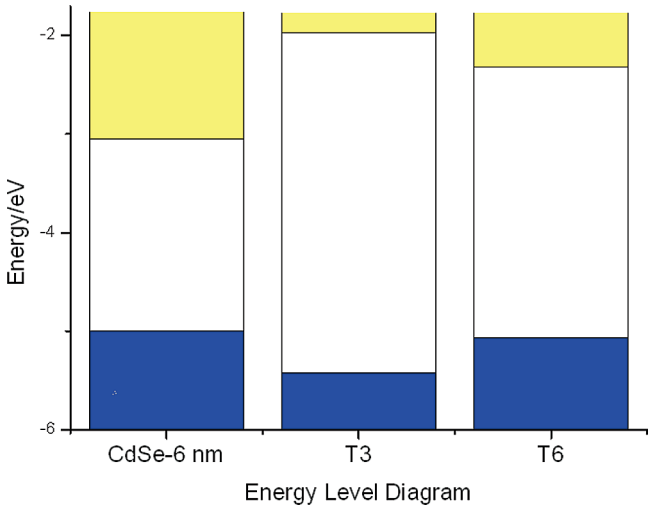

Oligothiophene- or polythiophene-nanocrystal complexes are novel building blocks for solar-cell fabrication. Thus phosphonate-ended oligomers with five thiophene rings or more may undergo photoinduced charge transfer with CdSe-NCs[12] and the complexes themselves could serve as the active material in a solar cell. As in CdSe-P3HT solar cells, both components absorb light, and electron transport can be controlled by nanocrystal shape.[5d] Advincula reports dendronized oligothiophenes (n = 3 and 7) capping CdSe-NCs with phosphonic acid ends.[7f] Linear oligothiophenes (n = 1−3) were linked to CdSe-NCs via the thiol end through replacement of capping tetradecylphosphonic acid[13] and their PL quenching was investigated. Terthiophenes bearing a carboxylic-acid moiety linked in α terminal position of their backbone through a linear alkyl chains have been used to cap CdSe-NCs and the PL quenching rate was found to decrease with the spacer length.[14]

Recent papers report P3HT-functionalization of TOPO-capped CdSe-NCs[15] for which solid-state emission spectra suggested charge transfer from P3HT to CdSe, P3HT thiol functionalization to CdSe-NCs for higher efficency of BHJ solar cells[16] and LB deposits of P3HT-CdSe nanocomposites used in a photovoltaic device.[17]

The interface between oligothophene and CdSe may be controlled on a molecular scale, so that a winning strategy to ease conduction may be that of creating oligothiophene surfactants that favor excited-state charge transfer when complexed to CdSe-NCs.

(6) (a) Sariciftci, N. S.; Smilowitz, L.; Heeger, A. J.; Wudl, F. *Science* **1992**, *258*, 1474. (b) Sariciftci, N. S.; Braun, D.; Heeger, A. J. *Appl. Phys. Lett.* **1993**, *62*, 585. (c) Halls, J. J. M.; Pichler, K.; Friend, R. H.; Moratti, S. C.; Holmes, A. B. *Appl. Phys. Lett.* **1996**, *68*, 3120. (d) Roman, L. S.; Andersson, M. R.; Yohannes, T.; Inganäs, O. *Adv. Mater.* **1997**, *9*, 1164. (e) Halls, J. J. M.; Arias, A. C.; MacKenzie, J. D.; Wu, W.; Inbasekaran, M.; Woo, E. P.; Friend, R. H. *Adv. Mater.* **2000**, *12*, 498. (f) Brabec, C. J.; Sariciftci, N. S.; Hummelen, J. C. *Adv. Funct. Mater.* **2001**, *11*, 15. (g) Coakley, K. M.; McGehee, M. D. *Chem. Mater.* **2004**, *16*, 4533. (h) Alam, M. M.; Jenekhe, S. A. *Chem. Mater.* **2004**, *16*, 4647.
(7) (a) Arango, A. C.; Carter, S. A.; Brock, P. J. *Phys. Rev. B* **2001**, *64*, 125 205. (b) Huynh, W. U.; Dittmer, J. J.; Teclemariam, N.; Milliron, D. J.; Alivisatos, P. A. *Phys.Rev.B.* **2003**, *67*, 115326. (c) Sun, B. E.; Max, E.; Greenham, N. C. *Nano Lett.* **2003**, *3*, 961. (d) Liu, J.; Kadnikova, E. N.; Liu, Y.; McGehee, M. D.; Fréchet, J. M. J. *J. Am. Chem. Soc.* **2004**, *126*, 9486. (e) Beek, W. J. E.; Wienk, M. M.; Janssen, R. A. J. *Adv. Mater.* **2004**, *16*, 1009. (f) Locklin, J.; Patton, D.; Deng, S.; Baba, A.; Millan, M.; Advincula, R. C. *Chem. Mater.* **2004**, *16*, 5187. (g) Lu, M.; Xie, B.; Kang, J.; Chen, F.-C.; Yang, Y.; Peng, Z. *Chem. Mater.* **2005**, *17*, 402. (h) Liu, J.; Tanaka, T.; Sivula, K.; Alivisatos, A. P.; Frechet, J. M. J. *J. Am. Chem. Soc.* **2004**, *126*, 6550. (i) Nozik, A. J. *Phys. E* **2002**, *14*, 115. (j) Robel, I.; Subramanian, V.; Kuno, M.; Kamat, P. V. *J. Am. Chem. Soc.* **2006**, *128*, 2385.
(8) Huynh, W. U.; Dittmer, J. J.; Alivisatos, A. P. *Science* **2002**, *295*, 2425.
(9) Zotti, G.; Vercelli, B.; Berlin, A. *Chem. Mater.* **2008**, *20*, 397.
(10) Greenham, N. C.; Peng, X.; Alivisatos, A. P. *Phys.Rev.B* **1996**, *54*, 17628.
(11) Kongkanand, A.; Tvrdy, K.; Takechi, K.; Kuno, M.; Kamat, P. V. *J. Am. Chem. Soc.* **2008**, *130*, 4007.
(12) Milliron, D. J.; Alivisatos, A. P.; Pitois, C.; Edder, C.; Fréchet, J. M. J. *Adv. Mater.* **2003**, *15*, 58.
(13) Sih, B. C.; Wolf, M. O. *J. Phys. Chem. C* **2007**, *111*, 17184.
(14) Pokrop, R.; Pamula, K.; Deja-Drogomirecka, S.; Zagorska, M.; Borysiuk, J.; Reiss, P.; Pron, A. *J. Phys. Chem. C* **2009**, *113*, 3487.
(15) Xu, J.; Wang, J.; Mitchell, M.; Mukherjee, P.; Jeffries-ElJacob, M.; Petrich, W.; Lin, Z. *J. Am. Chem. Soc.* **2007**, *129*, 12828.
(16) Palaniappan, K.; Murphy, J. W.; Khanam, N.; Horvath, J.; Alshareef, H.; Quevedo-Lopez, M.; Biewer, M. C.; Park, S. Y.; Kim, M. J.; Gnade, B. E.; Stefan, M. C. *Macromolecules* **2009**, *42*, 3845.
(17) Goodman, M. D.; Xu, J.; Wang, J.; Lin, Z. *Chem. Mater.* **2009**, *21*, 934.

Chart 1

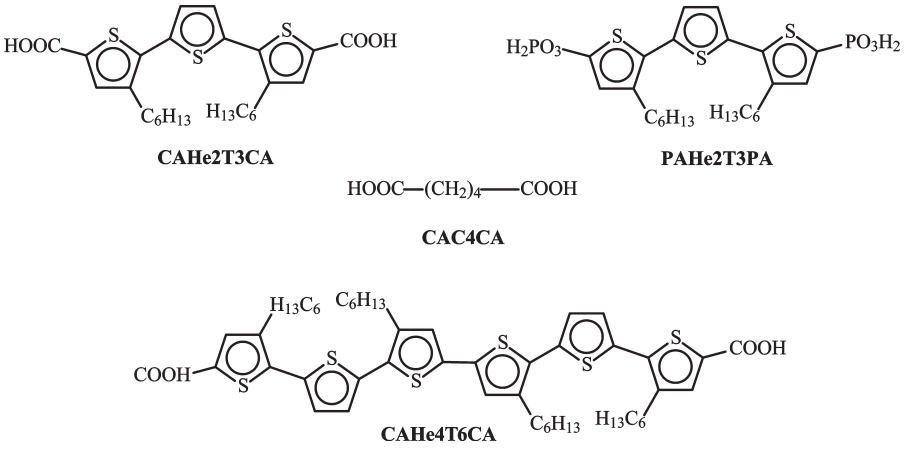

CAHe2T3CA **PAHe2T3PA**

CAC4CA

CAHe4T6CA

Chart 2

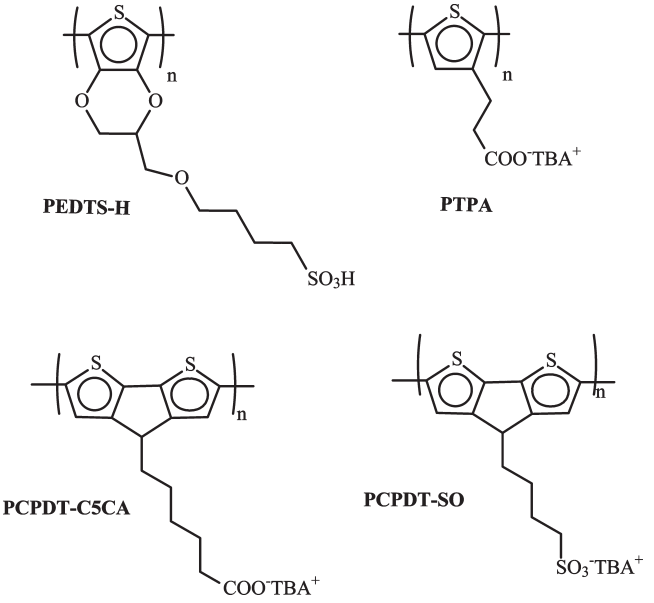

Our investigations point to satisfy the need for fast *electron and hole* transfer between the inorganic semiconductor nanoparticles through the organic bridge. In this report, we consider in particular p-type conduction, namely hole transport between adjacent oligothiophene-bridged CdSe-NCs upon photoexcitation. Charge injection energy levels are crucial for the conduction of these materials and appropriate matching must exist between the ionization potential (HOMO) of the CdSe-NCs and that of the oligothiophenes.

Typical CdSe-NCs of 6 nm diameter have an electron affinity (LUMO) of 3.05 eV and an ionization potential (HOMO) of 5.05 eV.[5a,18] As illustrated in Scheme 1, the energy levels of CdSe-NCs are nested between those of terthiophene (T3) but with sexithiophene (T6) the HOMO level is at the same energy of the CdSe HOMO, which is the best condition for efficient hole transport. For these reasons we selected T3 and T6 as model oligomeric linkers to be compared.

Soluble polythiophenes were also investigated for comparison. With these the nanoparticles are not linearly connected by conjugated bridges, as in the oligothiophenes, but they are pendant from polyconjugated polymer chains. The two different patterns should be characterized by different pathways for conduction.

The thiophene oligomers and polymers used for CdSe capping are shown in Charts 1 and 2. As far as the link is concerned, in agreement with previous work[12] and confirmed by our prevous investigation with polymers,[19] we selected carboxylic (mainly), sulfonic and phosphonic acids. They are most effective headgroup for functionalization of the colloidal CdSe surface since they bind more strongly than the ligands present in the synthetic starting product, namely, amines, thiols, phosphines, and phosphine oxides. These latter functionalities in the head of the surfactant are therefore permanently displaced. Moreover we introduced into the oligomers alkyl (hexyl) substituents in order to confer them, and particularly sexithiophene, a solubility in nonpolar solvents sufficiently high for the construction of multilayers (see below); the presence of the alkyl chains may in fact increase the distance between linkers, but not appreciably that between the linked particles.

Hexadecylamine-capped CdSe nanocrystals of 6 or 7.5 nm diameter were used since the red-shifted peak of such relatively large NCs allows the obtaining of optical responses well separated from those of the organic ligands. Moreover CdSe-NCs have a quantum yield over 50% upon hexadecylamine capping[20] so that PL changes may be best observed.

We used the layer-by-layer (LBL) method to assembly hybrid organic/CdSe multilayer thin films from nonaqueous solutions of oligothiophenes (as anionic bipolar amphiphiles) or polythiophenes (bearing anionic substituents aside the polyconjugated chain) and the hexadecylamine-capped CdSe nanocrystals. The resulting structure is schematically shown in Scheme 2. The same technique

(18) Colvin, V. L.; Alivisatos, A. P.; Tobin, J. G. *Phys. Rev. Lett.* **1991**, *66*, 2786.

(19) Zotti, G.; Vercelli, B.; Berlin, A.; Chin, P. T. K.; Giovanella, U. *Chem. Mater.* **2009**, *21*, 2258.

(20) (a) Qu, L.; Peng, X. *J. Am. Chem. Soc.* **2002**, *124*, 2049. (b) de Mello Donegá, C.; Hickey, S. G.; Wuister, S. F.; Vanmaekelbergh, D.; Meijerink, A. *J. Phys. Chem. B* **2003**, *107*, 489.

Scheme 2. Pictorial View of CdSe-NCs and Dicarboxylic-Ended Terthiophene in a Bridged Structure

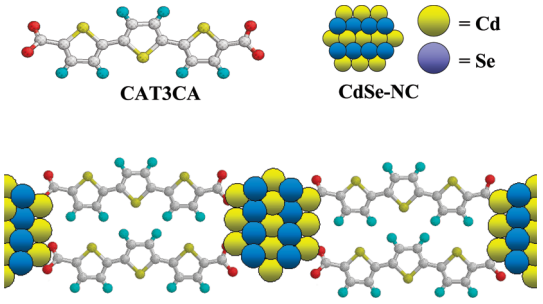

has been previously used for CdSe-NCs in alternation with poly(*p*-phenylenevinylene)s to form covalently bound layered structures.[21]

The multilayer buildup was monitored by UV−vis spectroscopy, and the new materials were investigated by cyclic voltammetry, UV−vis and FTIR spectroscopy, photoelectrochemistry, and photoconductivity. In the report, we first describe the way ligand substitution operates to link CdSe-NCs and carboxylate linkers, then we will report the construction of the layered structures on ITO from the monolayer to the multilayer, considering in details the electrochemical generation and transport of holes in ITO/linker/CdSe bilayers. Finally the photoluminescence, photoconductivity and photoelectrochemistry of the multilayers will be reported.

2. Experimental Section

2.1. Chemicals and Reagents. Acetonitrile was reagent grade (Uvasol, Merck) with a water content $< 0.01\%$. The supporting electrolyte tetrabutylammonium perchlorate (Bu_4NClO_4), poly(*p*-styrenesulfonic acid) (PSSH), poly(acrylic) acid (PAAH), adipic acid (CAC4CA), branched polyethylenimine (PEI), and all other chemicals were reagent grade and used as received.

Synthesis of oligothiophenes and polythiophenes can be found in details in the Supporting Information (SI). 5,5″-(3′,3″-Dihexyl-2,2′:5′,2″-terthiophene)-dicarboxylic acid (CAHe2T3CA) and (3′,3″-dihexyl-5″-phosphono-2,2′:5′,2″-terthiophene-5-yl)-phosphonic acid (PAHe2T3PA) were prepared starting from 3′,3″-dihexyl-2,2′:5′,2″-terthiophene (He2T3) and 5,5″-dibromo-3′,3″-dihexyl-2,2′:5′,2″-terthiophene respectively. CAHe4T6CA was prepared via anodic coupling of He2T3CA.

Poly(tetrabutylammonium 6-(4*H*-cyclopenta[2,1-*b*:3,4-*b*′]-dithien-4-yl)hexanoate) (PCPDT-C5CA)[22] and poly(tetrabutylammonium 4-(4*H*-cyclopenta[2,1-b:3,4-b′]dithien-4-yl)butanesulfonate) (PCPDT-SO)[23,24] were prepared by electrochemical oxidation of the corresponding monomers.

Poly(thiophene-3-propionic acid) (PTPA) with a degree of polymerization of ∼50 was produced according to McCullough[25] and used as the tetrabutylammonium salt. Poly(4-(2,3-dihydrothieno[3,4-*b*][1,4]dioxin-2-ylmethoxy)-butane-1-sulfonic acid) (PEDTS-H) was prepared according to the literature.[26]

Soluble CdSe-NCs with the surface capped by hexadecylamine and stearic acid were produced as detailed in SI. Two sizes of NCs were used, with absorption maxima at 623 and 648 nm, corresponding to an average size of 6.0 and 7.5 nm,[27] confirmed by TEM analysis. Absorbance and PL spectra in $CHCl_3$ are given in Figure S3 in the SI for the 6.0-nm sample. The PL maxima are characterized by a small Stokes shift (ca. 6 nm) and are narrow (ca. 25 nm at half width).

2.2. Substrates and Multilayer Film Formation. Transparent modified surfaces were prepared from glass sheets or indium−tin-oxide (ITO)/glass electrodes (20 Ω sq^{-1} from Merck-Balzers).

Monolayer formation of PAAH, CAC4CA, and PEI on ITO was performed as previously reported.[19]

The build-up of multilayers on ITO/glass electrodes was performed according to the methodology introduced by Decher,[28,29] that is, by dipping the electrodes alternatively into the solutions of the two components. After each immersion step, the substrate was carefully washed and dried in air. The layer build-up was monitored by UV−vis spectroscopy.

The concentration of CdSe-NCs dispersions in $CHCl_3$ used for layering was 10^{-3} M in CdSe units. The bipolar amphiphiles and the polymers PAAH and PSSH were used 10^{-3} M in EtOH solution (as monomeric units). For the polythiophenes, because of their scarce solubility in the acid form, they were used 10^{-3} M in the anionic form, namely, as the tetrabutylammonium salt, which is even more strongly acting toward ligand substitution.[30,31] Exposure time was 5 min in all cases.

2.3. Apparatus and Procedure. *2.3.1. Electrochemistry, Spectroscopy and Prophilometry*. Electrochemical experiments were performed in acetonitrile + 0.1 M Bu_4NClO_4, at room temperature and under nitrogen, using three electrode cells. The working electrodes for cyclic voltammetry (CV) of layers were 1 × 4 cm^2 ITO/glass sheets. The counter electrode was platinum; the reference electrode was a silver/0.1 M silver perchlorate in acetonitrile (0.34 V vs SCE, 4.77 V vs vacuum). The voltammetric apparatus (AMEL, Italy) included a 551 potentiostat modulated by a 568 programmable function generator.

UV−vis spectra were run on a Perkin-Elmer Lambda 15 spectrometer. FTIR spectra were taken in reflection−absorption mode on platinum sheets or in transmission on KBr pellets using a Perkin-Elmer 2000 FTIR spectrometer. Multilayer thicknesses were determined with an Alphas-step IQ prophilometer from KLA Tencor.

2.3.2. Photoluminescence. PL experiments were carried out at room temperature. The sample was optically pumped by the second harmonic (400 nm, duration pulse of around 50 fs) of a Ti/sapphire femtosecond laser system. The incident pulse energy was ∼1 μJ. A fiber bundle was placed close to the sample to collect the emitted light. Detection was performed using an Oriel Instaspec IV spectrometer with 1 nm spectral resolution.

(21) Liang, Z. Q.; Dzienis, K. L.; Xu, J.; Wang, Q. *Adv. Funct. Mater.* **2006**, *16*, 542.
(22) Berlin, A.; Zotti, G.; Schiavon, G.; Zecchin, S. *J. Am. Chem. Soc.* **1998**, *120*, 13453.
(23) Zotti, G.; Zecchin, S.; Berlin, A.; Schiavon, G.; Giro, G. *Chem. Mater.* **2001**, *13*, 43.
(24) Zotti, G.; Zecchin, S.; Schiavon, G.; Berlin, A.; Pagani, G.; Canavesi, A. *Chem. Mater.* **1997**, *9*, 2940.
(25) Ewbank, P. C.; Loewe, R. S.; Zhai, L.; Reddinger, J.; Sauve, G.; McCullough, R. D. *Tetrahedron* **2004**, *60*, 11269.
(26) Zotti, G.; Zecchin, S.; Schiavon, G.; Groenendaal, L. *Macromol. Chem. Phys.* **2002**, *203*, 1958.
(27) Yu, W. W.; Qu, L.; Guo, W.; Peng, X. *Chem. Mater.* **2003**, *15*, 2854.
(28) (a) Decher, G.; Hong, J. *Makromol. Chem. Macromol. Symp.* **1991**, *46*, 321. (b) Decher, G.; Hong, J. *Ber. Bunsenges. Phys. Chem.* **1991**, *95*, 1430. (c) Decher, G. *Science* **1997**, *277*, 1232.
(29) Ito, H.; Niimi, Y.; Suzuki, A.; Marumoto, K.; Kuroda, S. *Thin Solid Films* **2008**, *516*, 2743.
(30) Zotti, G.; Vercelli, B.; Berlin, A. Unpublished work.
(31) Kopping, J. T.; Patten, T. E. *J. Am. Chem. Soc.* **2008**, *130*, 5689.

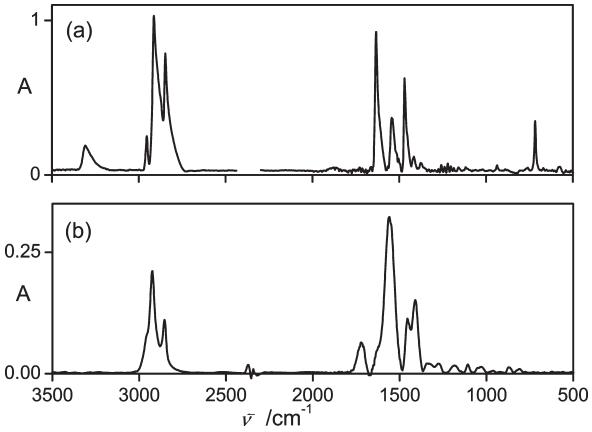

Figure 1. FTIR spectrum of CdSe-NCs (a) before and (b) after PAAH treatment.

2.3.3. Photoelectrochemistry and Photoconductivity. Photoelectrochemical experiments were performed in nitrogen-saturated aqueous 0.1 M NaBr using a three-electrode cell with a saturated calomel electrode (SCE) as a reference and a platinum counter electrode. All potentials and energies are given with respect to SCE, which is 4.43 eV below the vacuum level. The working electrode was illuminated on the solution side with a water-filtered 100 W halogen lamp, spotted over an area of ~10 cm^2. The resulting light power, calibrated with a silicon photodiode, was ~100 mW cm^{-2}. Light was chopped with a manually driven shutter.

Photoconductivity measurements of multilayers were performed with a special Hg electrode contacting the multilayer-covered ITO as described previously.[19] Bias was applied to ITO vs Hg electrode. Illumination (100 mW cm^{-2}) was performed as described above on the back glass side of the ITO/multilayer.

3. Results and Discussion

3.1. Full Carboxylate-Capping of CdSe-NCs. CdSe-NCs with an average diameter of 6.0 nm contain ~2000 CdSe units and a full ferrocene coverage of the surface (4×10^{-10} mol cm^{-2})[32] involves ~300 molecules on a single nanocrystal. The ratio of bulk (N_b) and surface (N_s) molecules is therefore $N_b/N_s = \sim 7$.

The occurrence of extensive surface ligand substitution has been checked with poly(acrylic acid) (PAAH). The polymer (1 mg) dissolved in THF (5 mL) was added to 8 mg of CdSe-NCs in 5 mL of $CHCl_3$ and reacted for some hours. After evaporation of the solvent and washing of the residue with ethanol, the residue had become insoluble in $CHCl_3$, indicating the cross-linking of the NCs occurred.

The FTIR spectrum of the product (Figure.1) shows the almost complete loss of the amine bands at 3300 and 1640 cm^{-1} and the strong enhancement of the band at 1560 cm^{-1} because of the COO^- asym stretching and of the corresponding weaker sym stretching band at 1407 cm^{-1}, whereas a band at 1720 cm^{-1}, because of free COOH moieties of PAAH, has appeared. In any case, the persistence of strong CH stretching bands around 2900 cm^{-1} indicates that the stearate ligands, originally present along with the hexadecylamine ligands, are essentially preserved. Through the use of oligothiophene-based carboxylate-ended molecules, it has also been possible to evaluate the ratio (~2:3) of initially surface-bound stearate and new carboxylate caps,.[30] It can be argued that the same amine displacement happens also with the carboxyl-functionalized molecules used throughout this study and, possibly, also with the phosphonate- and sulfonate-ended linkers.

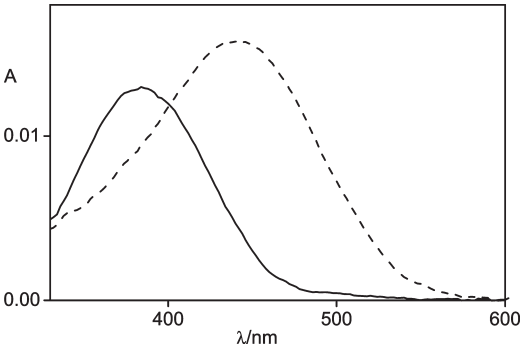

Figure 2. UV−vis spectra of (—) ITO/CAHe2T3CA and (--) ITO/CAHe4T6CA monolayers.

3.2. Oligothiophene-CdSe Structures. *3.2.1. Monolayers.* A monolayer of bipolar-amphiphile oligothiophene is formed on ITO-glass from ethanol solution as shown by UV−vis spectroscopy (Figure.2). For CAHe2T3CA, the UV−vis spectrum shows the T3 signal with maximum at 387 nm and absorbance of 13×10^{-3} au. The bathochromic shift from the $CHCl_3$ solution (374 nm) is attributable to a higher coplanarity of the thiophene rings in the solid state layers because of loss of solvent swelling the hexyl substituents. The absorbance value, using the extinction coefficient of 2.5×10^4 M^{-1} cm^{-1} for T3,[33] corresponds to a dense coverage of 2.6×10^{-10} mol cm^{-2}. For PAHe2T3PA, the T3 maximum is shown at 362 nm, and the absorbance is comparable (10×10^{-3} au, ~2×10^{-10} mol cm^{-2}).

The UV−vis spectrum of the CAHe4T6CA layer shows the T6 signal with maximum at 441 nm (vs 426 in $CHCl_3$) and absorbance of 16×10^{-3} au. Using the coefficient of 6×10^4 M^{-1}cm^{-1} for T6,[33] the coverage is 1.3×10^{-10} mol cm^{-2}, i.e. right half the value for the T3.

CV of the oligothiophene monolayers in acetonitrile[22] has shown the two-electron irreversible oxidation of CAHe2T3CA monolayer at $E_p = 1.0$ V (1.08 V for PAHe2T3PA) and the two-electron reversible oxidation of the CAHe4T6CA monolayer at $E^0 = 0.57$ and 0.77 V. The charge involved is 70 (100 for PAHe2T3PA) and 40 μC cm^{-2} respectively, that is, the amount of the T6 is approximately half of the T3, in line with the spectral results above. This fact may be attributed to the higher steric requirements of the T6 vs the T3 molecules on the surface, mainly attributable to the bulky hexyl substituents lateral to the oligothiophene rigid rod chain.

(32) Gui, J. Y.; Stern, D. A.; Lu, F.; Hubbard, A. T. *J. Electroanal. Chem.* **1991**, *305*, 37.

(33) Chosrovian, H.; Rentsch, S.; Grebner, D.; Dahm, D. U.; Birckner, E.; Naarmann, H. *Synth. Met.* **1993**, *60*, 23.

Table 1. Two-Side CdSe Exciton-Band (ΔA_{CdSe}) and Thiophene π-Band (ΔA_{Tn}) Differential Absorbance of Multilayers on ITO for 6.0-nm CdSe-NCs Using Different Linkers

linker	$\Delta A_{CdSe} \times 10^3$/au layer^{-1}	$\Delta A_{Tn} \times 10^3$/au layer^{-1}
CAHe2T3CA	3	10
PAHe2T3PA	3	13
CAHe4T6CA	3	15
PTPA (EtOH)	7	5
PTPA (CH_2Cl_2)	6	25
PCPDT-C5CA	5	12
PCPDT-SO	7	4
PAAH	2.5	-

A stable CdSe-NC monolayer is formed on top of the oligothiophene-primed ITO-glass when it is dipped in the NC dispersion. The limiting two-side absorbance of the first-exciton band of CdSe-NC monolayer is 2×10^{-3} au. Given a molar extinction coefficient of 6.6×10^5 $M^{-1}cm^{-1}$ for this size (6 nm) of the nanocrystals,[27] the coverage is 1.5×10^{-12} nanocrystal mol cm^{-2}. With 2000 CdSe units in the NC, this corresponds to 3×10^{-9} CdSe units mol cm^{-2}, that is, 10-fold the oligothiophene coverage, which indicates that a dense CdSe coverage is obtained.

3.2.2. Multilayers. Multilayers are built on the ITO electrodes with alternate exposure to the oligothiophene and CdSe solutions. UV−visible spectroscopy was used to monitor the assembling process of such LBL film and the obtained optical parameters are summarized in Table 1.

The absorption spectra of multilayer films prepared with different numbers of layers is shown in Figure.3. The observed linear increase of CdSe and oligothiophene absorbances vs the number of layers indicated a stepwise and uniform assembly process.

The two-side absorbance differential increase (ΔA) at 625 nm (because of CdSe, ΔA_{CdSe}) is 3×10^{-3} au layer^{-1}, that is, somewhat higher than for the starting monolayer (2×10^{-3} au layer^{-1}). This band is recorded at the same energy of the first exciton band of CdSe colloidal particles in solution. This indicates that the CdSe-NCs are successfully assembled without forming aggregates with directly contacting nanoparticles.

Considering the oligothiophene contribution to the layers, the differential T3 absorbance at 380 nm (ΔA_{Tn}) is $(10-13) \times 10^{-3}$ au layer^{-1} whereas the T6 differential absorbance (ΔA_{Tn}) at 440 nm is 15×10^{-3} au layer^{-1}. From the extincion coefficients it results that the T6 linker molecules are roughly half those found in the T3 case, which parallels the lower molar coverage of T6 vs T3 monolayers reported above.

3.3. Polythiophene-CdSe Structures. *3.3.1. Monolayers.* A monolayer of the polycyclopentadithiophenes is formed on ITO-glass from $(2-4) \times 10^{-4}$ M solution in 3:1 ethanol/water as shown by UV−vis spectroscopy (Figure.4). The spectrum shows the polythiophene signal with maximum at 500 nm and absorbance of $(5-7) \times 10^{-3}$ au. The maximum wavelength corresponds to a degree of polymerization of ~5 (10 thiophene rings),[22] that is, in fact to a short oligomeric mixture. The absorbance values, using the extinction coefficient of 1.2×10^4 $M^{-1}cm^{-1}$,[23] correspond to a dense coverage of $(2-3) \times 10^{-10}$ mol cm^{-2} (as monomeric units).

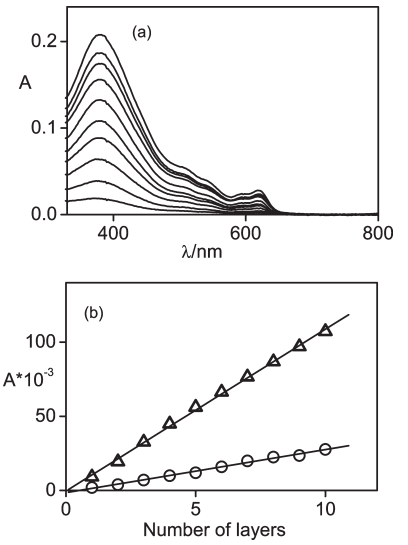

Figure 3. (a) UV−vis spectra of ITO/(CAHe2T3CA/CdSe)$_n$ multilayers (n = 1−10) and (b) relevant plots of (O) CdSe and (Δ) CAHe2T3CA absorbances vs n. Spectra are background-corrected.

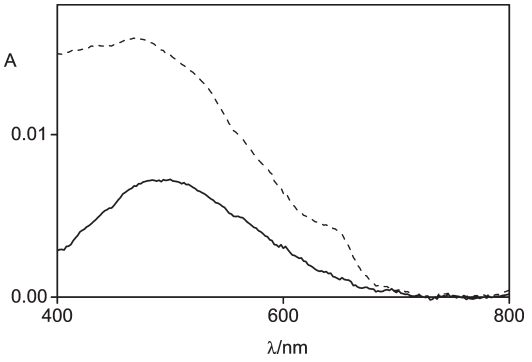

Figure 4. UV−vis spectra of (—) ITO/PCPDT-C5CA and (- -) ITO/PCPDT-C5CA/CdSe layers.

The regioregular polythiophene PTPA forms a similar monolayer on ITO-glass from 4×10^{-4} M solution in CH_2Cl_2 or EtOH. The UV−vis spectrum shows the polythiophene signal with maximum at 450 nm, that is, with no shift from the solutions,[25] and absorbance of 24×10^{-3} and 4×10^{-3} au, respectively. The absorbance value, using the extinction coefficient of 0.8×10^4 M^{-1} cm^{-1}, corresponds to a coverage of 15×10^{-10} and 2.5×10^{-10} mol cm^{-2} (as monomeric units). Thus the polarity of the solvents is crucial for the amount of adsoption. In any case, adsorption from a solvent of intermediate polarity like acetonitrile yields the same coverage of EtOH, so that it appears that two discrete situations are achieved.

The different levels of PTPA adsorption in different solvents may be accounted for by a different orientation of the polythiophene rigid-rod chains on the ITO surface, namely, with the axis over the ITO plane and the thiophene plane either parallel or perpendicular to the ITO plane. The former case will force a low density of adsorbed thiophene rings, comparable with that of ferrocene,[32]

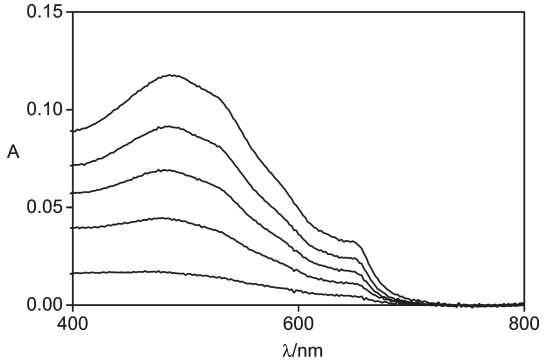

Figure 5. UV−vis spectra of ITO/(PCPDT-C5CA/CdSe)$_n$ multilayers (n = 1−5). Spectra are background-corrected.

whereas the latter will allow the chains to be stacked side by side with a much higher density. A similar behavior has been previously observed in the oligothiophene- and oligopyrrole-mediated aggregation of gold nanoparticles.[34] Moreover it is possible that this behavior is apparent with PTPA right because of its stereoregularity coupled with solubility in different solvents, as found in OFETs based on regioregular poly(3-hexylthiophene).[35] In that case self-organization has given a lamella structure with two-dimensional conjugated sheets formed by interchain stacking and, depending on processing conditions, the lamellae can adopt two different orientations, parallel and normal to the substrate.[35]

Also in this case a stable CdSe monolayer is formed on top of the polythiophene-primed ITO-glass by dipping in the 7.5-nm CdSe NC dispersion. Its spectrum (Figure.4) shows, in addition to the strong band of the polythiophene, the CdSe exciton band at 650 nm with an absorbance of 7×10^{-3} au.

3.3.2. Multilayers. As for oligothiophenes, multilayers are built on ITO surfaces with alternate exposure to polythiophene and CdSe dispersions and the obtained optical parameters are summarized in Table 1.

The absorption spectra of multilayer films prepared with different numbers of layers are shown in Figure.5. The observed linear increase of CdSe (at 650 nm) and polythiophene (at 500 or 450 nm depending on the polymer) absorbances vs the number of layers indicates a stepwise and uniform assembly process.

The two-side differential absorbance increases (ΔA) for PCPDT-C5CA, corrected for the overlapping of spectra, are $\Delta A_{CdSe} = 5 \times 10^{-3}$ and $\Delta A_{Tn} = 12 \times 10^{-3}$ au layer^{-1}, which are considerably higher (by a factor of ca. 1.7) then those measured for the first layer. This result must be attributed to the higher exposed area of the layers beyond the first one.

In the case of PCPDT-SO, the ΔA_{CdSe} and ΔA_{Tn} values (7×10^{-3} and 4×10^{-3} au layer^{-1}) indicate a growth rate for CdSe similar with that for PCPDT-C5CA but a much (3 times) lower growth rate for the polymer. This result, which finds a confirmation in the higher thickness of the PCPDT-C5CA vs PCPDT-SO layers (6 vs 2 nm layer^{-1}, see Table 2), may be accounted for by the different characteristics of the carboxylate and sulfonate terminal functionalities, since the former are more likely to be present as the protonated form, able to interact via H-bonding with others in neighbor polymer chains. This may produce aggregation of polymeric chains to form multiple layers, rather than monomolecular layers, between the CdSe-NCs in the growing composite multilayer.

Table 2. Total (d) and Differential (d_0) Thickness of Some Multilayers for CdSe-NCs of Various Diameter (∅) and Different Linkers

multilayer	CdSe∅/nm	d/nm	d_0/nm layer^{-1}
(CAHe2T3CA/CdSe)$_{10}$	6.0	28 ± 2	3
(CAHe4T6CA/CdSe)$_{10}$	6.0	34 ± 3	3
(PTPA/CdSe)$_5$ (EtOH)	7.5	32 ± 2	6
(PTPA/CdSe)$_5$ (CH_2Cl_2)	7.5	48 ± 4	10
(PCPDT-C5CA/CdSe)$_{10}$	7.5	63 ± 1	6
(PCPDT-SO/CdSe)$_5$	7.5	22 ± 2	4

For PTPA-based multilayers grown in EtOH the normal linear increase of the CdSe exciton band (once more 7×10^{-3} au layer^{-1}) is accompanied by a modest increase of the PTPA band (5×10^{-3} au layer^{-1}). In contrast, in CH_2Cl_2 the polymer growth is massive. The observed linear increase of CdSe (at 650 nm) and polythiophene (at 460 nm) absorbances is 6×10^{-3} and 25×10^{-3} au layer^{-1}, respectively. The data, compared with those (5×10^{-3} and 12×10^{-3}) of PCPDT-C5CA, indicate a comparable growth of the CdSe component but a double contribution from the polythiophene component.

3.4. Thickness of Multilayers. AFM examination has shown that the multilayers are very uniform; moreover they are robust enough to stand a standard sticky-tape test without appreciable losses. Their thickness has been measured and results are summarized in Table 2.

The (oligothiophene/CdSe)$_n$ structures display a differential thickness of ∼3 nm layer^{-1}. Compared with the theoretical thickness of ∼5 nm layer^{-1} for a compact hexagonal arrangement of the 6-nm nanocrystals,[19] the value is indicative of a lower mass contribution by each layer because the oligomers compared with the polymers.[19]

In fact (polythiophene/CdSe)$_n$ multilayer, for example, (PCPDT-C5CA/CdSe)$_{10}$ with 7.5-nm CdSe-NCs, has shown 60 nm thickness in perfect agreement with the calculated value. Also PTPA-based multilayers are thick, and those from CH_2Cl_2 are much thicker then those from EtOH (10 vs 6 nm layer^{-1}) in agreement with spectral analysis. PCPDT-SO/CdSe multilayers are moderately thinner, as expected on the basis of the spectral analysis.

We must finally recall that polymer sublayers are in general very thin. Thus in a typical alternate deposition of poly(stirenesulfonate) and protonated poly(allylamine), performed in the absence of added salt, the average thickness of each polymer sublayers is 0.5−0.6 nm only.[36]

(34) Zotti, G.; Vercelli, B.; Berlin, A.; Battagliarin, M.; Hernández, V.; López-Navarrete, J. T. *J.Phys.Chem.C* **2007**, *111*, 5886and refs therein .
(35) Sirringhaus, H.; Brown, P. J.; Friend, R. H.; Nielsen, M. M.; Bechgaard, K.; Langeveld-Voss, B. M. W.; Spiering, A. J. H.; Janssen, R. A. J.; Meijer, E. W.; Herwig, P.; de Leeuw, D. M. *Nature* **1999**, *401*, 685.
(36) Lvov, Y.; Decher, G.; Mohwald, H. *Langmuir* **1993**, *9*, 481.

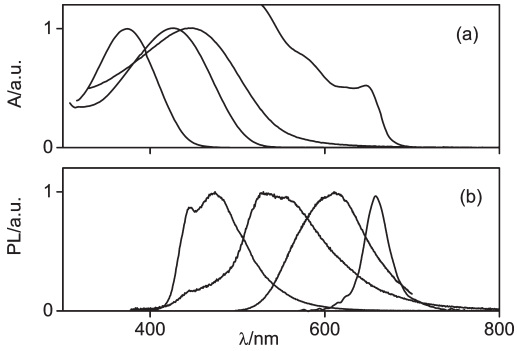

Figure 6. Absorbance (a) and PL (b) spectra of (from left) CAHe2T3CA, CAHe4T6CA. PTPA and 7.5-nm CdSe-NCs. Absorbance in $CHCl_3$ solution and PL as film, except PTPA (both in EtOH).

Table 3. PL Intensity I_{PL} for Multilayers (7.5-nm CdSe-NCs, λ_{PL} = 653 nm) Relative to $(PVPY/CdSe)_{10}$ Multilayer (4.0-nm CdSe-NCs, λ_{PL} = 600 nm)

multilayer	I_{PL}
$(PVPY/CdSe)_{10}$	1.00
$(CAHe2T3CA/CdSe)_5$	0.25
$(CAHe4T6CA/CdSe)_5$	0.02
$(PTPA/CdSe)_5$ (EtOH)	0.40
$(PTPA/CdSe)_5$ (CH_2Cl_2)	1.40
$(PCPDT\text{-}SO/CdSe)_5$	0.90
$(PCPDT\text{-}C5CA/CdSe)_5$	0.09
$(PCPDT\text{-}C5CA/CdSe)_{10}$	0.20

It is for this reason that ruler of the thickness of the reported layers is the NC size.

3.5. PL Spectroscopy of Multilayers. The PL spectra of oligothiophenes, polythiophenes, and 7.5-nm CdSe-NCs in solution are shown in Figure.6, along with the corresponding absoption spectra. The intensity of PL emission is high, both for the organic and the inorganic components.

In spite of this, under 400 nm excitation, involving both the oligo(poly)thiophene and the CdSe components, the PL of multilayers show only the CdSe-NC exciton component. The PL intensities, relative to that of a polyvinylpyridine-CdSe multilayer with 10% QY[19] taken as a reference, are summarized in Table 3.

The $(oligothiophene/CdSe)_n$ multilayers emit significantly (~25% of the reference) in the case of the T3, whereas the emission is low (less than 2−3%) for the T6 case. This result confirms those obtained in an analogous PL experiment where T3 and T5 were compared.[12]

Polythiophene-based multilayers are in general emissive with an intensity comparable with that of the polypyridine-CdSe reference multilayer. The only exception is the case of PCPDT-C5CA layers, for which the emission is ca. 10-times less intense, probably attributable to the higher oligothiophene content. PTPA multilayers from EtOH emit much less than the multilayers from CH_2Cl_2, due to the massive presence of the polythiophene in the latter. The action of the polythiophene on the PL properties of the Cd-NCs is currently under detailed investigation.

3.6. Electrochemistry of ITO/Oligothiophene/CdSe layers. As evidenced in the formation of LBL multilayer described above, a stable CdSe-NC monolayer is formed

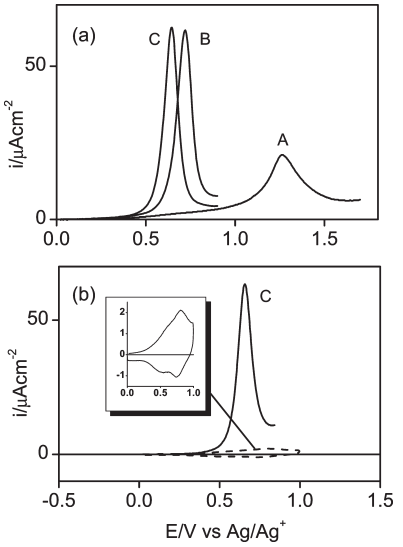

Figure 7. (a) Voltammograms of (A) ITO/CAC4CA/CdSe, (B) ITO/CAHe2T3CA/CdSe, and (C) ITO/CAHe4T6CA/CdSe layers and (b) voltammograms of (--) ITO/CAHe4T6CA and (—) ITO/CAHe4T6-CA/CdSe layers in acetonitrile + 0.1 M Bu_4NClO_4. Scan rate: 0.02 V s^{-1}.

Scheme 3. Electrochemical Oxidation of CdSe-NCs with (a) Tetramethylene and (b) Sexithiophene Spacers

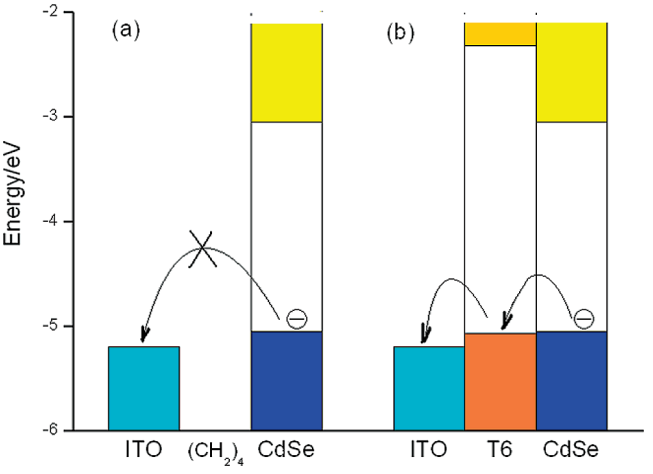

on top of the oligothiophene-primed ITO-glass, giving a two-sublayer sandwich structure.

The CV of such sandwich electrode is expected to show the oxidation processes of both the oligothiophene and the CdSe-NC sublayers. In fact oxidation of 6.0-nm CdSe NCs fixed on a nonelectroactive ITO/CAC4CA monolayer (Figure.7a) displays the previously reported oxidation process at E_p = 1.25 V because of the two-electron oxidation of all the CdSe units in the nanocrystal.[19] The charge involved is ~0.4 mC cm^{-2}. When the T6 moiety is interposed between the ITO and the CdSe-NCs, the reversible two-electron process of the T6 moiety is overcome by the intense oxidation of the CdSe, anticipated to E_p = 0.64 V (Figure.7b). The same happens with the T3 moiety, for which the anticipation is only slightly lower (E_p = 0.72 V) whereas the onset of oxidation is the same at ~0.3 V (Figure.7a).

These results are accounted for by the availability of holes for conduction in the T6 and T3 moieties at

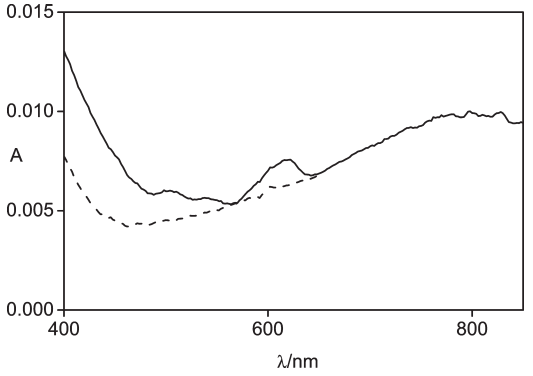

Figure 8. UV−vis spectra of (- -) ITO/PEI/PEDTS-H and (—)ITO/PEI/PEDTS-H/CdSe layers.

potentials close to the CdSe valence band (Scheme 3). In this way the CdSe oxidation, which is positively shifted to 1.25 V in an insulating bridge such as the CAC4CA (four methylene moieties $-(CH_2)_4-$) may occur at potentials closer to the thermodinamic energy value because of the presence of holes in the sexithiophene bridge. With the T3, which has the valence band at a lower energy (see energy diagram in Scheme 1), the process occurs after oxidation of the T3 at a higher potential, that is, with ~0.1 V anodic potential shift from than in T6. We have to consider that though the CAC4CA spacer (0.8 nm in the extended conformation) is much shorter than CAHe4T6CA (2.7 nm) the absence of empty orbitals at the CdSe HOMO level makes such a spacer an obstacle to charge hopping.

The occurrence of CdSe oxidation at a thermodynamically defined energy level (electrode potential) has been evidenced by the use of conducting PEDT as bridge between the CdSe-NCs and the ITO electrode. This polymer is in fact conducting through a band encompassing the HOMO energy edge of CdSe and which can be continuously modulated by an applied potential.[37] Such a sandwich layer has been produced with a monolayer of PEDT sulfonate, that is, PEDTS-H,[26] fixed on a ITO/PEI surface from 10^{-3} M solution in water/ethanol, over which a CdSe-NCs monolayer was fixed through the external sulfonate ends. The UV−vis spectra of ITO/PEI/PEDTS-H and ITO/PEI/PEDTS-H/CdSe layers, shown in Figure.8, evidence the formation of the PEDTS and CdSe layers as a broad absorption and an exciton absorption respectively. CV (Figure.9) shows that the flat capacitive response of PEDT continues until the CdSe-NCs are oxidized at a potential (E_p = 0.72 V) close to those of the thiophene oligomers. The CdSe oxidative discharge waits until the PEDT valence band is depleted to the level of the CdSe HOMO, as predicted. In fact the used CdSe-NCs of 6 nm diameter have a band gap of 2.00 eV[5a] separating an electron affinity of 3.05 eV and an ionization potential of 5.05 eV. The latter HOMO value corresponds to ~0.3 V vs Ag/Ag^+, which is approximately the onset of CdSe oxidation in the oligothiophene-CdSe layers (Figure.7).

(37) Groenendaal, L.; Zotti, G.; Aubert, P. H.; Waybright, S. M.; Reynolds, J. R. *Adv. Mater.* **2003**, *15*, 855.

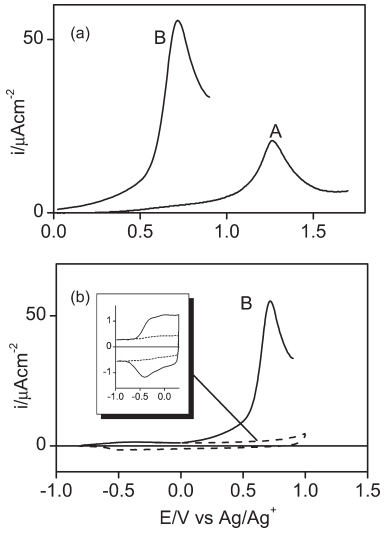

Figure 9. (a) Voltammograms of (A) ITO/CAC4CA/CdSe and (B) ITO/PEI/PEDTS-H/CdSe layers and (b) voltammograms of (- -) ITO/PEI/PEDTS-H and (—)ITO/PEI/PEDTS-c/CdSe layers in acetonitrile + 0.1 M Bu_4NClO_4. Scan rate: 0.02 V s^{-1}.

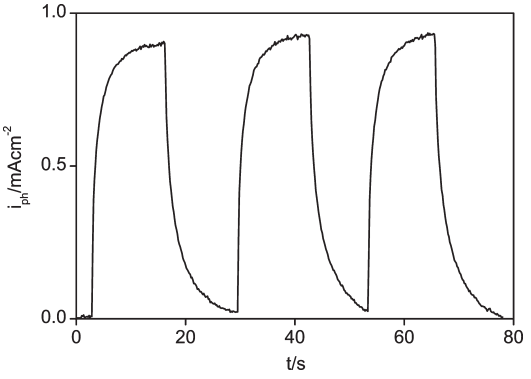

Figure 10. Photocurrent transient for $(PCPDT\text{-}C5CA/CdSe)_{10}$ (7.5-nm CdSe) multilayer on ITO.

The results reported in this section evidence that the availability of a p-doped hole-conducting bridge eases charge transport, which may be true also for an improved hole photoconduction. This is the object of the photochemical investigations reported in the following sections.

3.7. Photoconductivity of Multilayers. Measurements at 1 V and 100 mW cm^{-2} illumination produce photocurrent transients like those illustrated in Figure 10. Results for different multilayers are summarized in Table 4.

$(PAAH/CdSe)_{10}$ and $(PSSH/CdSe)_{10}$ multilayer with the 6.0-nm CdSe-NCs have given a photocurrent of 4−10 mA cm^{-2}, in line with previous results on 3−5 nm diameter CdSe-NCs.[19] Surprisingly we found that $(oligomer/CdSe)_{10}$ multilayers are not photoconductive, which may be attributed to the spacers being much longer than the polymer thickness. In other words the decrease in photoconductivity is predominantly caused by the increase in NC spacing.

In contrast with oligomers, the photoconductivities of polythiophene multilayers are high. In $(PTPA/CdSe)_5$ multilayers, the thin-spaced multilayers (from EtOH)

Table 4. Solid-State Photocurrents i_{ph} (at 1 V Applied Potential at 0.023 cm^2 ITO-Hg Contacts) and Photocurrent Onset Potentials E_{on} (in 0.1 M NaBr) for Multilayers under 100 mW cm^{-2} Illumination[a]

multilayer	A/au	i_{ph}/mA cm^{-2}	E_{on}/V vs SCE
$(CAHe2T3CA/CdSe)_{10}$	0.030	< 0.05	−0.25
$(PAHe2T3PA/CdSe)_{10}$	0.025	< 0.05	0.40
$(CAHe4T6CA/CdSe)_{10}$	0.030	< 0.05	0.30
$(PCPDT-C5CA/CdSe)_{10}$	0.060	1	0.20
$(PCPDT-C5CA/CdSe)_5$	0.030	2	0.20
$(PCPDT-SO/CdSe)_5$	0.035	6.5	−0.65
$(PTPA/CdSe)_5$ (EtOH)	0.030	4	−0.70
$(PTPA/CdSe)_5$ (CH_2Cl_2)	0.030	0.4	−0.70
$(PAAH/CdSe)_{10}$	0.025	10	−0.05
$(PSSH/CdSe)_{10}$	0.040	4	−0.70

[a] Two-side exciton-band absorbance A is also given.

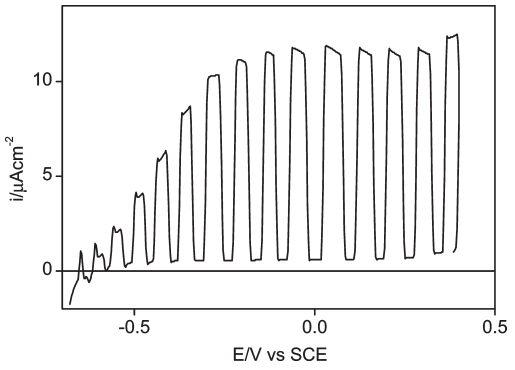

Figure 11. Photoelectrochemical $i-V$ plot for ITO/$(PTPA/CdSe)_5$ multilayer in 0.1 M NaBr. Scan rate: 0.005 V s^{-1}.

are highly photoconductive, like PAAH-spaced samples, whereas the thick-spaced multilayers (from CH_2Cl_2) display a 10-times lower, albeit still noticeable, photoconductivity. It appears that in polymers the disposition of the polythiophene chains makes the interdot distance lower than in oligothiophenes, thus easing charge transport.

3.8. Photoelectrochemistry of Multilayers. To better understand the photoconductive properties of the multilayers and in consideration of CdSe-NCs applications in photoelectrochemical cells,[11] we have investigated their photoelectrochemical behavior. Photoelectrochemical analysis of charge-transport in multilayers was investigated in a cell containing nitrogen-fluxed 0.1 M NaBr.

A typical $i-V$ curve in response to chopped illumination (100 mW cm^{-2}), presented in Figure.11, shows the generation of anodic photocurrent. Anodic photocurrents increased with increasing anodic polarization sloping up to a plateau value.

The response does not produce photodegradation of the layers, as evidenced by the UV−vis spectra which show both the CdSe and the oligo(poly)thiophene responses unchanged after the photoelectrochemical test. This means that photoxidation concerns the electrolyte and not the semiconductors themselves. Moreover, since the responses are practically the same with nonoxidizable anions (such as in 0.1 M $NaClO_4$) and in the thiophene-free $(PAAH/CdSe)_n$ multilayers, the process must be the photoxidation of water and photogeneration of current is located in the CdSe component solely. The photoelectrochemical process is illustrated in Scheme 4.

Scheme 4. Photoelectrochemical Oxidation of Water by CdSe-NC Multilayers

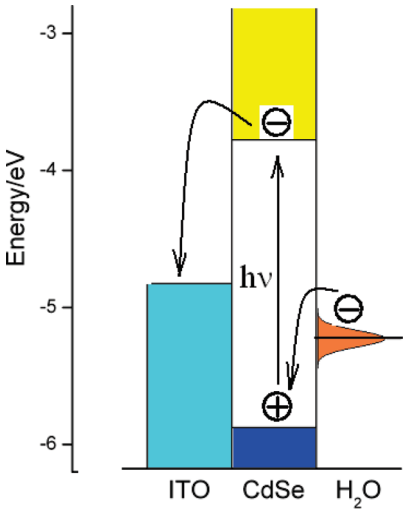

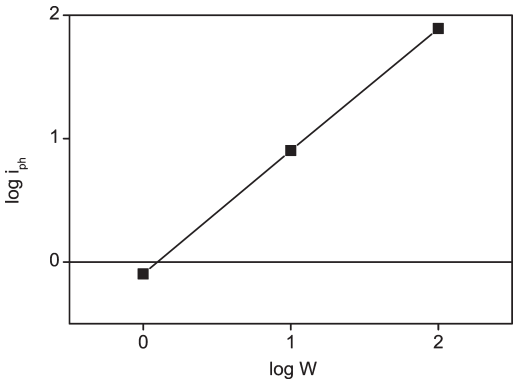

Figure 12. Log−log plot of photocurrent i_{ph} vs illumination power W of ITO/$(PCPDT-SO/CdSe)_5$ multilayer in 0.1 M NaBr.

In the plateau region of the $i_{ph}-V$ curves control is operated by the photocurrent generation. This is shown by the dependence from the CdSe content of the multilayer, since plateau values are ~10 and 20 μA cm^{-2} for multilayers composed by $n = 5$ and 10 CdSe layers respectively. Moreover the photocurrent responses i_{ph} increase linearly with the incident illumination power W (in the range 1−100 mW cm^{-2}) with a linear log−log plot sloping unity (Figure.12) as sign of no appreciable recombination of photocarriers.[29]

On the contrary the photocurrent-onset potentials, given in Table 4, are quite sensitive to the ligand type.

3.8.1. Oligothiophene-Based Multilayers. We consider first the oligothiophene-based multilayers compared with $(PAAH/CdSe)_{10}$. The responses of PAAH and CAHe2T3CA are similar (Figure.13), the only difference being in practice the onset potential (−0.05 and −0.25 V vs SCE respectively), which may simply be due to different locations of the band edges originating from the different moieties connected to the carboxylate ends. The case of CAHe4T6CA is surprising since the onset potential, which should in principle have been the same of CAHe2T3CA, is anodically shifted to ~0.3 V (Figure.13), and the response has a steeper increase with voltage. The

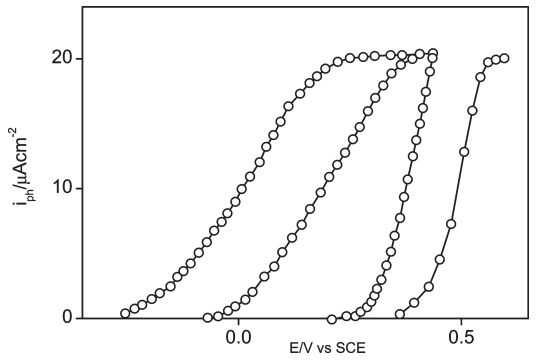

Figure 13. Photoelectrochemical $i_{ph}-V$ curves of ITO/(linker/CdSe)$_{10}$ multilayers for linkers (from left) CAHe2T3CA, PAAH, and CAHe4T6-CA and PAHe2T3PA in 0.1 M NaBr. Scan rate: 0.005 V s^{-1}.

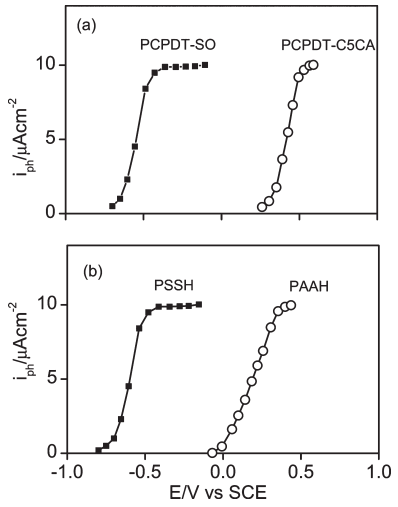

Figure 14. Photoelectrochemical $i_{ph}-V$ curves of CdSe-multilayers (n = 5) based on (a) PCPDT-SO (left) and PCPDT-C5CA (right) and (b) PSSH (left) and PAAH (right) in 0.1 M NaBr. Scan rate: 0.005 V s^{-1}.

possibility that at this photocurrent onset a significant presence of oxidized CAHe4T6CA linkers may act as charge-transfer mediators must be ruled out since CA-He4T6CA is oxidized at a much higher potential (0.66 V vs SCE) so that the photoconduction must involve charge transport across nonoxidized T6 moieties.

The responses of PAHe2T3PA is similar to that of CAHe2T3CA but the onset potential is strongly positive (0.4 V vs SCE, 0.6 V more positive) because of a stabilization of the band edges by the strongly nucleophilic phosphonate ends. The highly positive voltages cause in any case a marked degradation of the layer, in correspondence of a noticeable dark current.

3.8.2. Polythiophene-Based Multilayers. In (polythiophene/CdSe)$_n$ multilayers, the polymer chains, that is, the polythiophene linear rods, are disposed parallel to the CdSe surface. As shown by Table 4 and in Figure.14a, the CPDT-based layers show strongly different onset potentials, which must be attributed to the different coordinating (sulfonate and carboxylate) side ends of the polymer chains. Most surprisingly the nonthiophene-based polysulfonate and polycarboxylate (PSSH and PAAH, Figure.14b) behave the same way. Moreover the regioregular PTPA, which provides the lowest onset potential of the thiophene series, and PSSH show the same onset albeit the latter operates without the help of thiophene rings. These are the final confirmations that the thiophene conjugated chains exert no action on the photoactivity of these layers, paralleling the photoconductive properties in the solid state reported above.

3.8.3. Photoelectrochemical Dynamics. Photocurrent generation at semiconductor nanoparticles is believed to occur via a mechanism different from the corresponding bulk semiconductors. For semiconductor nanoparticles, their small size makes band-bending and space-charge region not applicable. Instead, spatial confinement in the nanoparticles causes the photogenerated electron and hole wave functions to extend to the nanoparticle surface and into the medium rendering both carriers instantly available at the surface. The control of charge transport between multilayers appears therefore to be located at the linkers and dominated by the hopping distance, that is, the spacing length. Considering the carboxylic terminals, such length is comparable for PAAH and CAHe2T3CA but much longer for CAHe4T6CA. Thus an overvoltage higher than 0.5 V is required to activate charge transport along the T6 moiety and this is a clear indication that a long spacer, albeit highly conjugated, is in fact an obstacle to hole photoconduction.

Considering the energy levels of the investigated system, namely, the band edges of the CdSe-NC layer and the energy level of water oxidation, it results that the water oxidation potential at neutral pH is located in proximity of the valence band of the CdSe-NCs. Thus photoxidation of water through removal of photoexcited electrons in the CdSe conduction band (as illustrated in Scheme 4) may be performed only with a positive bias of the ITO contact higher than the Fermi level of CdSe-NC (~4 eV or −0.5 V vs SCE). This in fact occurs at potentials of −0.7 V or higher (see Table 4) depending on the linker. Positive overvoltages are required to overcome the activation energy for charge transport along the linker connections and therefore onset voltages are an indirect measures of the photoconductivity of the layers.

3.8.4. Conjugation and Spacing in Conduction. Electrogenerated holes in the oligo(poly)thiophene Tn has shown to be effective in easing electron transport between CdSe-NCs. In contrast, photogenerated holes in the CdSe-NCs cannot take advantage of the Tn bridges, as if no appreciable hole injection is operating. The apparent discrepancy may be accounted for by the chemical changes, including anion insertion and molecular conformational variation, produced by oxidation of Tn bridges, which does not take place in the photogeneration of holes in the solid-state semiconductor.

Thus the Tn linkers in the solid state behave simply as spacers and control charge transfer by their length only. Analogously in CdS-NCs, tethered to TiO_2 nanoparticles through bifunctional mercaptoalkanoic acids of different lengths, the yield of electron injection from photoexcited CdS-NCs to TiO_2 nanoparticles decreases with

increasing mercaptoalkanoic chain length and interparticle separation.[38]

4. Conclusions

A series of anion-functionalized oligothiophenes and polythiophenes were combined with hexadecylamine-capped CdSe nanoparticles to form regular multilayers via solution processing. The new structures, constituted by quantum dots linked by hole-transporting conjugated chains, display optical and electronic properties useful in photovoltaic devices.

The most striking outcome of this investigation is that charge transport between dots is in fact eased by the conjugated linker chains in electrochemical arrangements, but in the solid state, transport of photogenerated carriers is dominated by interdot distance with no help from conjugation. In particular the PL quenching observed in sexithiophene and not in terthiophene linkers, which could have suggested an enhanced photogeneration of carriers,[39] has in fact proved of no relevance to the effective photoconductivity.

Such a drawback may in principle be overcome by the use of linkers which, instead of acting as bridges for holes, may favor transport of electrons. New materials of this type are actually investigated actively in our laboratories.

Acknowledgment. The authors would like to thank S. Sitran of the CNR for his technical assistance.

Supporting Information Available: Synthesis of oligothiophenes, polythiophenes, and nanocrystals. This material is available free of charge via the Internet at http://pubs.acs.org.

(38) Dibbell, R. S.; Watson, D. F. *J. Phys. Chem. C* **2009**, *113*, 3139.
(39) Asokan, S.; Krueger, K. M.; Alkhawaldeh, A.; Carreon, A. R.; Mu, Z. Z.; Colvin, V. L.; Mantzaris, N. V.; Wong, M. S. *Nanotechnology* **2005**, *16*, 2000.